General Disclaimer

One or more of the Following Statements may affect this Document

- This document has been reproduced from the best copy furnished by the organizational source. It is being released in the interest of making available as much information as possible.

- This document may contain data, which exceeds the sheet parameters. It was furnished in this condition by the organizational source and is the best copy available.

- This document may contain tone-on-tone or color graphs, charts and/or pictures, which have been reproduced in black and white.

- This document is paginated as submitted by the original source.

- Portions of this document are not fully legible due to the historical nature of some of the material. However, it is the best reproduction available from the original submission.

9

GA-9495

A Facsimile Report

Reproduced by
UNITED STATES
ATOMIC ENERGY COMMISSION
Division of Technical Information
P.O. Box 62 Oak Ridge, Tennessee 37830

SQT-63927R

Gulf General Atomic
Incorporated
P. O. Box 608, San Diego, California 92112

GA-9495

SOME INVESTIGATIONS OF REFRACTORY METAL SYSTEMS OF THERMIONIC INTEREST*

by

R. G. Hudson, M. H. Horner and L. Yang

This paper was presented at the
1969 IEEE Thermionic Conversion Specialist Conference
October 21-23, 1969, Carmel, California

*This work was sponsored partly by the
National Aeronautics and Space Administration
under Contracts NAS 3-4165 and NAS 3-8504
and partly by the
Atomic Energy Commission
under Contract USAEC AT(04-3)-167,
Project Agreement 14

Projects 552 and 4022

November, 1969

SOME INVESTIGATIONS OF REFRACTORY METAL SYSTEMS OF THERMIONIC INTEREST*

R. G. Hudson, M. H. Horner and L. Yang

ABSTRACT

Interdiffusion of the W-Ta, W-Mo and W-Nb systems was studied in the temperature range 2000-2200°C. The diffusion rate was found to be in the order of W-Ta < W-Mo < W-Nb. For a diffusion time of 100 hours, the widths of the diffusion zone deduced from the concentration distribution curves of the samples studied were: (1) 2000°C – 39, 88 and 130 microns; (2) 2100°C – 77, 118 and 301 microns; and (3) 2200°C – 134, 164 and 486 microns; for the W-Ta, W-Mo and W-Nb systems respectively. In all the cases studied, the concentration distribution curves were unsymmetrical with respect to the Matano interface, and the diffusion constants deduced from these curves by using the Boltzmann-Matano method increased with the increase of the Ta, Mo or Nb concentration. Kirkendall voids were observed on the Ta, Mo or Nb side of the interface in systems studied at 2000°C, but very few or no voids were found in systems studied at 2200°C. Pre-treatment at 2200°C for 100 hours was found to reduce the number of Kirkendall voids formed at a W-Ta interface upon subsequent heating at 1650°C for 400 hours.

Planar emitter structures were prepared by diffusion bonding W emitters of 40 mil thickness to Ta-10W substrates. After these emitter structures were operated in cesiated converters at 1427° to 1575°C for 2000-4000 hours, their vacuum work functions were measured and then the widths of the

*This work was sponsored partly by the National Aeronautics and Space Administration under Contracts NAS 3-4165 and NAS 3-8504 and partly by the Atomic Energy Commission under Contract USAEC AT(04-3)-167, Project Agreement 14.

diffusion zones at the W to Ta-10W interfaces were determined. The diffusion zones varied from 30 to 80 microns in thickness. There was no indication that their vacuum work functions were affected by such interdiffusion.

Measurements were made on the vacuum work functions of W-2Mo, W-5Re and W-25Re alloys at 1800°C. The W-2Mo alloy emitted essentially like Mo with a vacuum work function of 4.39 eV. The W-5Re alloy which was provided by Oak Ridge National Laboratory, yielded a vacuum work function of 4.69 eV. The W-25Re alloy which was procurred from Cleveland Refractory Metals had a slight {110} preferred orientation and yielded a vacuum work function of 4.77 eV.

INTRODUCTION

In a thermionic converter, the emitter structure usually consists of a refractory metal emitter bonded to another refractory metal support. The electron work function of the emitter and the interdiffusion between the emitter and the support are of primary concern, since the emitter work function controls the converter output, while the interdiffusion between the emitter and the support may affect the structural integrity of the bond and the emitter work function. The following describes the results obtained on the interdiffusion of the W-Ta, W-Mo and W-Nb systems at high temperatures and the vacuum emission studies of W-(Ta-10W) emitter structures which have been operated for long periods of time in cesiated converters. Results on the vacuum work functions of some tungsten alloys are also included.

INTERDIFFUSION OF W-Ta, W-Mo AND W-Nb SYSTEMS

1. Experimental Techniques

The vacuum arc-melted tungsten and molybdenum rods were obtained from Climax Molybdenum Company and the electron beam melted tantalum and niobium rods were obtained from Wah Chang Corporation. Right cylinders of 1/4 inch by 1/4 inch were obtained from these rods and annealed in vacuum for 3 hours

at the intended diffusion temperature. Nine diffusion couples, designated as F_1 through F_9, were prepared from these annealed cylinders by diffusion bonding in vacuum at 1650°C and 1000 psi for 3 hours. Metallographic and electron microprobe examinations of the interface indicated perfect bond with interpenetration of less than a few microns in all cases. The couples were diffusion-annealed at 2000°C, 2100°C, and 2200°C for 100 hour each in a high temperature resistance furnace. The temperature of the furnace was measured with a calibrated optical pyrometer and controlled to ±15°C. After the completion of the diffusion-anneal, the samples were mounted in plastic and polished to expose the interface near the center of the cylinders. The distribution of the concentrations of the components across the interface was then determined by electron microprobe analysis. The results obtained were corrected for absorption to yield quantitative concentration penetration curves across the interface. After the completion of the electron microprobe scan of the interface, the microstructures of the interface were studied metallographically.

2. Experimental Results

(1) Concentration Penetration Curve. – The concentration penetration curves for Samples F_1 through F_9 are shown in Fig. 1 through 9. The Matano interfaces, defined by the relation

$$\int_0^{100} x\, dc = 0,$$

(where x is the distance from the Matano interface and c is the concentration of Ta, Nb, or Mo in wt-%), which are used as reference planes for the evaluation of the chemical diffusion constants, are also shown in these figures. It can be seen that all these curves are nonsymmetrical with respect to the Matano interface, indicating variation of the chemical diffusion constant with concentration because of the difference of the mobilities of the atoms of the two components of the couple.

(2) Microstructures at the Interface. – The microstructures at the interfaces of these diffusion couples are shown in Figs. 10 through 18. At 2000°C, pores are observed near the interface at the side of the lower-melting component (i.e., Ta, Nb, or Mo) of the couple. The formation of

such pores is believed to be due to the coalescence of lattice vacancies left behind when atoms of the faster-diffusing, lower-melting components crossed the interface at higher rates than that of tungsten atoms diffusing in the opposite direction. It is interesting to note, however, that in the Ta-W case at 2000°C, pores are absent at the interface of some crystal grains (see Fig. 10(b)). The exact reason for the dependence of pore formation upon interfacial crystal orientation is unknown. Perhaps defect concentrations, stress conditions, and impurity contents all play a part in determining the nucleation and growth of these pores.

As the diffusion temperature was increased, the concentration of pores at the interface decreased or even disappeared. Thus, at 2200°C no pores were observed at the Ta-W interface and very few pores were present at the Nb-W and the Mo-W interfaces. Moreover, it seems that the higher the melting point of the metal coupled with tungsten, the lower the temperature at which pore-free interface can be obtained. Thus, the Ta-W interface becomes pore-free at 2100°C, while for the Mo-W and the Nb-W interfaces, this condition is realized only at a higher diffusion temperature of 2200°C.

(3) Diffusion Coefficient and Activation Energy for Diffusion. – The diffusion coefficients D_c as a function of concentration at 2200°C, 2100°C, and 2000°C for the Ta-W, Nb-W, and Mo-W systems were evaluated from Figs. 1 through 9 by using the Boltzmann-Matano method according to the relationship derived from Fick's first law for D_c as a function of concentration

$$D_c = -\frac{1}{2t}\frac{dx}{dc}\int_{c_i}^{c} x\,dc,$$

where D_c is the diffusion coefficient in cm^2/sec at concentration c, x is the distance in centimeters perpendicular to the Matano interface, t is the diffusion time in seconds, and c_i is the reference concentration, which is 100% for the present case. The calculated D_c values are plotted as a function of concentration in Figs. 19, 20, and 21. It can be seen that D_c increases with the increase of the concentration of the low-melting component in all the three systems studied. Of all the D_c values at equivalent concentrations, the D_c values of the Nb-W system are the highest, while those

of the Ta-W system are the lowest, except at high tantalum and molybdenum concentrations and at high temperatures, where the D_c values of the Ta-W and the Mo-W systems are of the same order of magnitude. The D_c values obtained for the Nb-W system are about four orders of magnitude smaller than the values determined by microhardness measurements for the same system at the same temperature.(1) Such a discrepancy is probably due to the difference in the methods used for determining the penetration curve; the electron microprobe method is believed to be more accurate than the microhardness method. However, the results at 2100°C are in good agreement with that reported by Hehemann and Leber.(2)

In Figs. 22, 23, and 24, the D_c values are plotted versus the reciprocal of the absolute temperature. From the slopes of these plots, the activation energy values Q for the diffusion process are calculated and shown with the corresponding plots. Among the three systems studied, the Mo-W system has the smallest activation energy of diffusion.

(4) Width of Diffusion Zone. – The width of the diffusion zone is of practical significance to diffusion bonding. If the diffusion zone is arbitrarily defined as the region between 2 wt% Ta, Mo, or Nb and 98 wt% Ta, Mo, or Nb, then its width for 100 hour diffusion at 2000°, 2100°, and 2200°C can be measured directly from the penetration curves shown in Figs. 1 through 9. The data obtained are shown in Table 1. Included in the table are the widths of the diffusion zone for 10,000 hour diffusion at these temperatures, which are calculated from the 100 hour data on the basis of the square-root-of-time law. Of these three systems, the change of the width of the diffusion zone with temperature for a given time of diffusion is the least for the Mo-W system.

(5) Effect of High Temperature Pretreatment to Kirkendall Void Formation Upon Subsequent Annealing at Low Temperature. – Figure 25 shows the interface of a W-Ta couple which has been heated in vacuum at 1650°C for 400 hours. Numerous Kirkendall voids have been formed on the tantalum side of the interface. Figure 26 shows the interface of a W-Ta couple which was pretreated at 2200°C for 100 hours before being annealed at 1650°C for

400 hours. The number of Kirkendall voids is drastically reduced. Thus pretreatment at 2200°C to form a "graded interface" appears to be able to maintain a better bond upon subsequent operation at a lower temperature.

VACUUM EMISSION STUDY OF W-(Ta-10W) EMITTER STRUCTURE AFTER OPERATION IN CESIATED CONVERTERS

Planar emitter structures consisting of various types of tungsten emitters of 40 mil thickness diffusion-bonded (1850°C, 2000 psi, 3 hours) to Ta-10W substrates were prepared for the evaluation of their performances in cesiated converters. Upon the completion of the tests, the emitter structures were recovered and their vacuum work functions were determined in a vacuum emission cell of the type described in a previous paper.(3) After the vacuum emission study, each emitter structure was sectioned and the micro-structures and the composition distribution of the W-(Ta-10W) interface were examined by metallography and electron microprobe analysis. Figure 27 shows a typical photomicrograph of the post-test W-(Ta-10W) interface. The results on vacuum work function and diffusion zone width are summarized in Table 2. The vacuum work functions obtained are similar to those of the same type of emitter materials, studied previously,(6) indicating that the observed degree of interdiffusion between the tungsten emitter and the Ta-10W substrate did not seem to affect the vacuum work function of the emitter significantly.

VACUUM WORK FUNCTION OF SOME TUNGSTEN ALLOYS

Measurements were made on the vacuum work function of W-2Mo, W-5Re and W-25Re at 1800°C. The W-2Mo sample and the W-5Re sample were arc-cast material, obtained from Oregon Metallurgical Company and Oak Ridge National Laboratory* respectively. The W-25Re sample was of powder metallurgy origin, procurred from Cleveland Refractory Metals. X-ray studies indicated that no preferred crystal orientation existed in the W-2Mo and the W-5Re samples but the W-25Re sample had a very weak (110) preferred crystal orientation.

*Courtsey of A. C. Schaffhauser.

The W-2Mo sample emitted essentially like molybdenum, with a vacuum work function of 4.39 eV. Figure 28 shows the microstructures of the surface of this sample. Electron microprobe study showed, however, that molybdenum was barely detectable in very small areas widely scattered over the emitting surface and that within 12 microns from the emitting surface the molybdenum concentration dropped sharply. The depletion of molybdenum concentration of the emitting surface was probably due to the preferential vaporization of molybdenum over tungsten. However, the emitting surface must be covered with an adsorbed molybdenum layer which determined the vacuum work function.

The W-5Re sample and the W-25Re sample yielded vacuum work functions of 4.69 eV and 4.77 eV respectively. The W-5Re result agrees with that given in the review paper by Matskevich.(4) The W-25Re results also agrees with that given in the review paper by Matskevich, and falls within the range of values measured by Jacobson and Hamerdinger.(5) Figures 29 and 30 show the microstructures of the surfaces of the W-5Re sample and the W-25Re sample respectively. Study of the distribution of the rhenium concentration in these samples is in progress.

REFERENCES

(1) E. Gebhardt and K. Kirner, Z. Metallk. 54, 437 (1963).

(2) R. F. Hehemann and S. Leber, Trans. AIME. 236, 1040 (1966).

(3) R. G. Hudson and L. Yang, "Effect of Operating Temperature on the Vacuum Emission Stability of Vapor-Deposited Tungsten Clad UC-ZrC and UO_2," Proceeding of the Thermionic Specialist Conference, p. 212, Houston Texas, November 2-4, 1966. GA-7340.

(4) T. L. Matskevich, Soviet Physics-Technical Physics, 13, No. 3 p. 295, September 1968.

(5) Thirdly Quarterly Progress Report, Contract 952217, EOS Report 4006-Q-3, February 3, 1969.

(6) L. Yang and R. G. Hudson, "Effect of Preferred Crystal Orientation and Surface Treatment on the Work Function of Vapor-Deposited Tungsten," Proceeding of the Thermionic Specialist Conference, p. 395, Houston, Texas, November 2-4, 1966. GA-7343.

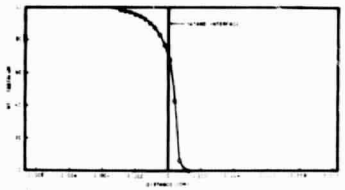

Fig. 1--Penetration curve for the tantalum-tungsten diffusion couple at 2000°C for 100 hr.

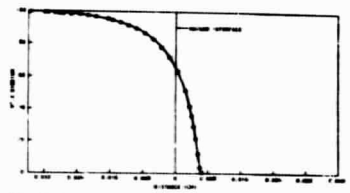

Fig. 5--Penetration curve for the niobium-tungsten diffusion couple at 2100°C for 100 hr.

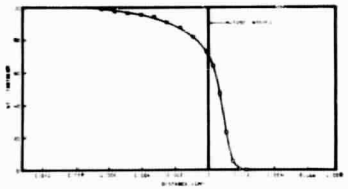

Fig. 2--Penetration curve for the tantalum-tungsten diffusion couple at 2100°C for 100 hr.

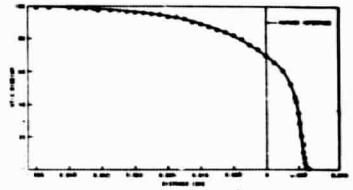

Fig. 6--Penetration curve for the niobium-tungsten diffusion couple at 2200°C for 100 hr.

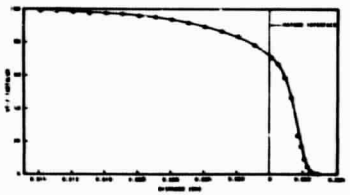

Fig. 3--Penetration curve for the tantalum-tungsten diffusion couple at 2200°C for 100 hr.

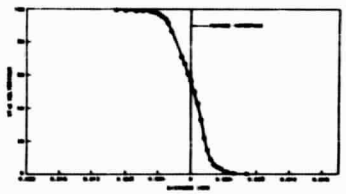

Fig. 7--Penetration curve for the molybdenum-tungsten diffusion couple at 2000°C for 100 hr.

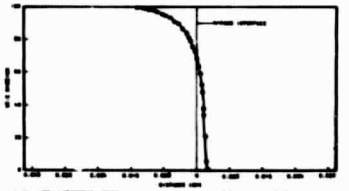

Fig. 4--Penetration curve for the niobium-tungsten diffusion couple at 2000°C for 100 hr.

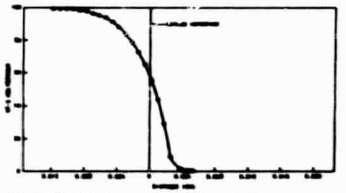

Fig. 8--Penetration curve for the molybdenum-tungsten diffusion couple at 2100°C for 100 hr.

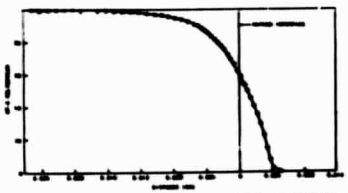

Fig. 9--Penetration curve for the molybdenum-tungsten diffusion couple at 2200°C for 100 hr.

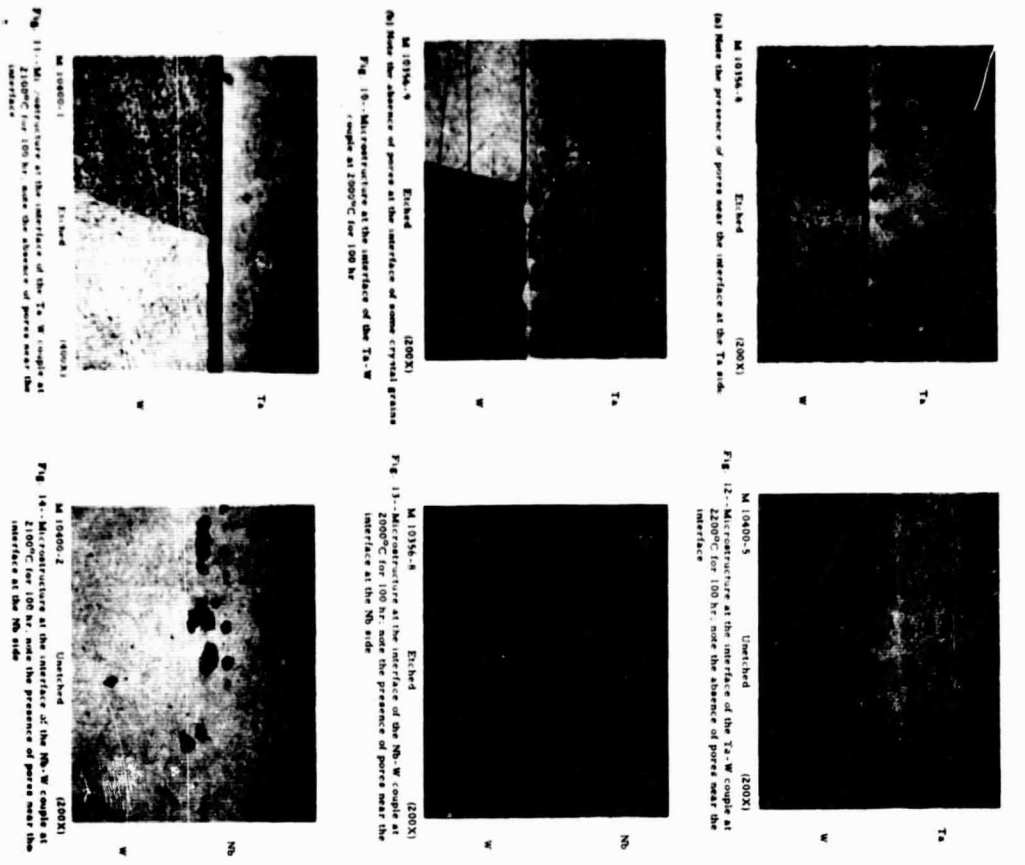

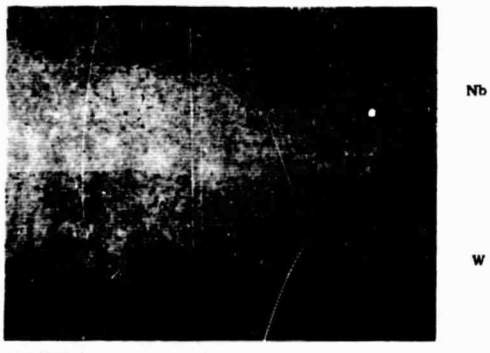

M 10400-6 Unetched (200X)

Fig. 15--Microstructure at the interface of the Nb-W couple at 2200°C for 100 hr; note the presence of very few pores near the interface

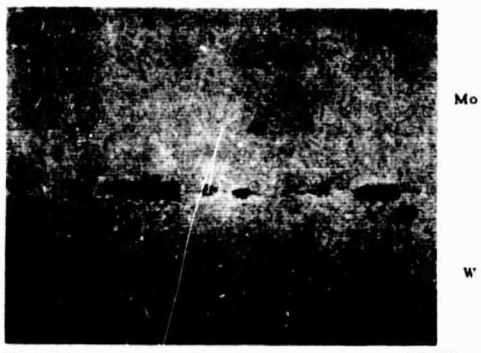

M 10400-4 Unetched (200X)

Fig. 17--Microstructure at the interface of the Mo-W couple at 2100°C for 100 hr; note the presence of pores near the interface at the Mo side

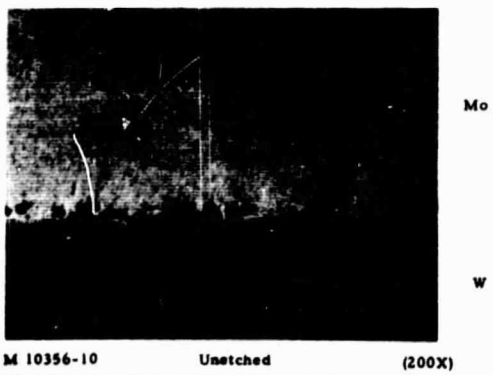

M 10356-10 Unetched (200X)

Fig. 16--Microstr cture at the interface of the Mo-W couple at 2000°C for 100 hr; note the presence of pores near the interface at the Mo side

M 10400-7 Unetched (200X)

Fig. 18--Microstructure at the interface of the Mo-W couple at 2200°C for 100 hr; note the presence of very few pores near the interface

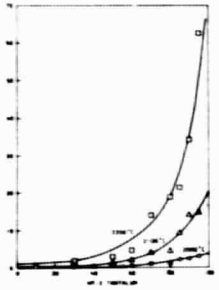

Fig. 19--Diffusion coefficient versus tantalum concentration for the tantalum-tungsten diffusion couple

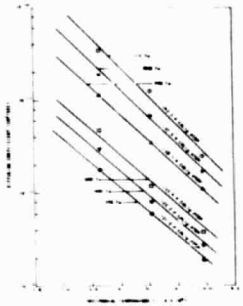

Fig. 22--Log of diffusion coefficient versus reciprocal absolute temperature for the tantalum-tungsten diffusion couple at various tantalum concentrations; activation energies are shown for each concentration

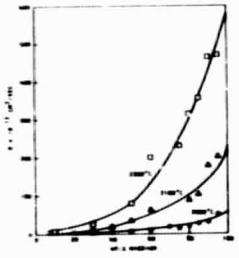

Fig. 20--Diffusion coefficient versus niobium concentration for the niobium-tungsten diffusion couple

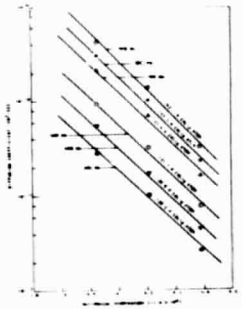

Fig. 23--Log of diffusion coefficient versus reciprocal absolute temperature for the niobium-tungsten diffusion couple at various niobium concentrations; activation energies are shown for each concentration

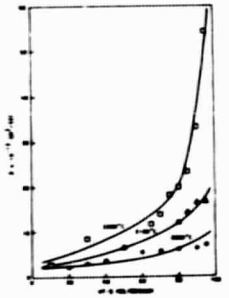

Fig. 21--Diffusion coefficient versus molybdenum concentration for the molybdenum-tungsten diffusion couple

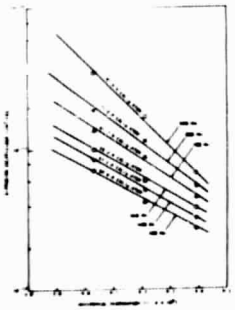

Fig. 24--Log of diffusion coefficient versus reciprocal absolute temperature for the molybdenum-tungsten diffusion couple at various molybdenum concentrations; activation energies are shown for each concentration

M 20471-1 100X

Fig. 25--Appearance of a W-Ta interface after 400 hours at 1650°C

M 27086-4 100X

Fig. 28--Microstructures of the surface of the W-2Mo sample after vacuum emission test

M 20471-2 100X

Fig. 26--Appearance of a W-Ta interface pre-treated at 2200°C for 100 hours and then heated 400 hours at 1650°C

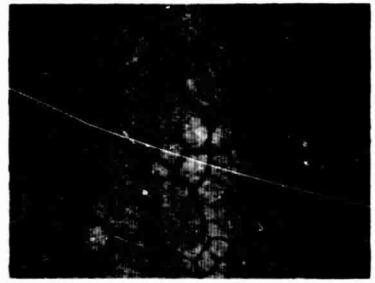

M 30838-1 100X

Fig. 29--Microstructures of the surface of the W-5Re sample after vacuum emission test

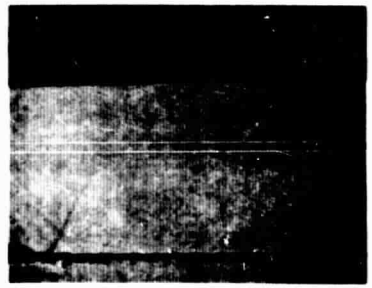

M 29919-3A 50X

Fig. 27--Appearance of the W-(Ta-10W) interface of emitter structure C_1-4 after 4000 hour test at 2000°K in a cesiated converter

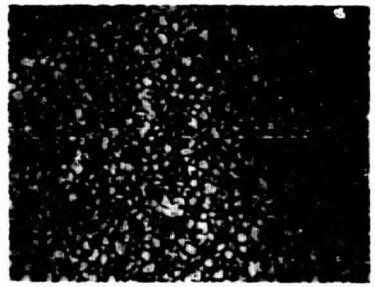

M 30837-1 100X

Fig. 30--Microstructures of the surface of the W-25Re sample after vacuum emission test

Table 1

DIFFUSION-ZONE WIDTH OF VARIOUS TUNGSTEN-REFRACTORY METAL DIFFUSION COUPLES FOR 100 HOURS AND FOR 10,000 HOURS[a]

Type of Couple	Temp. (°C)	Observed Width of Diffusion Zone in 100 Hr (microns)	Calculated Width of Diffusion Zone in 10,000 Hr[b] (microns)
Tantalum-Tungsten	2000	39	390
	2100	77	770
	2200	134	1340
Molybdenum-Tungsten	2000	88	880
	2100	118	1180
	2200	164	1640
Niobium-Tungsten	2000	130	1300
	2100	301	3010
	2200	486	4860

[a]The width of the diffusion zone is taken between 2 wt% and 98 wt% tantalum, molybdenum, or niobium.

[b]The calculated width of the diffusion zone for 10,000 hr is based on the assumption that the observed width in 100 hr obeys the square-root-of-time law.

Table 2

VACUUM WORK FUNCTION AND DIFFUSION ZONE WIDTH OF SOME PLANAR EMITTER STRUCTURES AFTER TESTING IN CESIATED CONVERTERS

Emitter Structure Designation	Testing Temperature (°K)	Testing Time (Hours)	Emitter	Substrate	Post-test Vacuum Work Function (eV)	Diffusion Zone Width* (microns)
B_6-1	2000	3000	Fluoride tungsten	Ta-10W	-	50
C_1-2	2030	3600	Chloride tungsten	Ta-10W	5.0	78
C_1-4	2000	4000	Chloride tungsten	Ta-10W	4.91	55
C_1-5	2000	4000	Chloride tungsten	Ta-10W	4.91	50
C_3-3	2000	4000	Chloride-fluoride duplex tungsten	Ta-10W	4.84	40
D_1-1	1700 1800 1900	250 350 1600	Etched fluoride tungsten	Ta-10W	4.77	27

*Arbitrarily defined as the distance between 2 wt% Ta and 88 wt% Ta on the concentration penetration curve.